Hydrodynamics of the flow of two immiscible liquids in a coiled tube of small diameter

S. Verma, V. Chauhan, S. Bharti, M. M. Mandal[*]

University School of Chemical Technology, Guru Gobind Singh Indraprastha University, N. Delhi, India

The present experimental study was carried out to investigate the hydrodynamics of two immiscible liquids (kerosene and water) flowing with superficial velocity ranging from 0.04 m/s to 0.4 m/s in a coiled tube. The effects of different flow rates of the immiscible liquids, oil volume fraction and curvature ratio of coiled tube on the pressure drop across the tube were investigated. It was also intended to observe the effect of T and Y mixer on the pressure drop of the kerosene-water flow through the coiled tube. Various patterns of flow such as stratified, dispersed, as well as annular were observed during the experimental campaign. Knowledge of flow pattern characterization is valuable for design and optimization of liquid-liquid transportation processes. This study shows that the proper control of these process parameters will help in controlling the energy losses in different equipment used in industries.

Keywords: oil-water flow, coiled tube, flow patterns, superficial velocity, pressure drop

INTRODUCTION

Literature survey shows that there has been an emerging trend in research on the oil-water flows in pipes and newer, greener technologies are being investigated to tackle the concerns for depleting oil reserves. The oil refineries are focusing to explore and process more viscous and heavier oil as they have more reserves worldwide in comparison to conventional oil [1]. Flow of two immiscible liquids is considered to be a multiphase flow and finds its relevance in various macro as well micro scale applications. These applications include flow of oil water through pipes with large diameter during oil drilling and transportation [2, 3], coolants for microfluidic conduits [4], process industries for reaction, extraction, emulsification, separation, etc. [5, 6]. It has been reported that volume fraction of water and temperature have no significant effect on pressure losses for a water-dominated flow. The water-dominated flow may be preferred during the transportation of heavy crude oil with water. The results establish a theoretical basis for water-lubricated transport of extra heavy crude oil [2]. A new drilling technology, i.e. coiled tubing ultra-short radius radial drilling has already been functional since late twentieth century [3]. This drilling technology has increased well productivity and reduced operating cost significantly as compared to conventional sidetrack drilling. It is also suitable for the productivity enhancement of old oilfields. Recently, this type of liquid-liquid flow has found its significance in micro-systems such as microreactors and micro-mixers which are designed and optimized for such systems. Currently, studies on fluid flow and heat transfer behavior of liquid–liquid two-phase flows are being carried out by various researchers to significantly improve the heat transfer rates in microchannels [4]. In all these applications, the behavior of the liquid-liquid immiscible flow was observed to be dissimilar to the flow of a single-phase liquid. These systems also demonstrate differences as compared to other type of multiphase flows such as gas–liquid flows and solid–liquid flows [7].

Knowledge on flows of immiscible liquids finds its use in tubular reactors employed in chemical, petrochemical, food, pharmaceutical and fine chemical industry where continuous processes take place. The diameters of these reactors could be in the range of millimetres. Many models have been proposed by different researchers which help in predicting the pressure gradient in straight pipes [8, 9]. Different models may be suited to predict pressure losses for different flow patterns. For example, a two-fluid model may be employed for stratified flow, whereas a homogeneous model may be used for dispersed flow [10]. A recent investigation on the flow pattern of a highly viscous oil–water flow at various temperatures in a straight tube has been reported [11]. It has been found that flow patterns of viscous oil–water flows are highly affected by temperature, oil fraction, as well as mixture velocity. It has also been reported that inversion points are intensely affected by mixture velocity.

* To whom all correspondence should be sent:
E-mail: monishamridha1@gmail.com

Pressure losses are found to vary from minimum to maximum at the inversion point [12].

Tubular reactors such as coiled tubes offer certain benefits in contrast to continuously stirred tank reactors. Recently, a coiled flow inverter (CFI) reactor was used for transesterification of fatty acids at various flow rates and residence times [13]. CFI also displayed twelve times faster biodiesel production than the conventional batch reactors at the given conditions. This was because of mixing enhancement which affected the contact between the liquid phases in the liquid-liquid reaction. The coiled reactors exhibit better heat transfer, mass transfer as well as control owing to improved compact size [14,15]. These types of reactors also reduce the possibility of hazards because of better temperature control and offer higher yields [16]. A good design of a reactor involves a considerable knowledge of the liquid-liquid flows through the pipes. A better understanding of the flow pattern is one of the parameters needed to know the hydrodynamics of the reactor. This further helps in measuring the interfacial area of contact between the liquids [17].

The motivation for this study was aroused when the literature review showed that the majority of the researches on liquid-liquid flows were confined to flows through straight tube and capillaries [18-22]. Studies on flow patterns have rarely been reported for coiled tubes [16, 23]. Moreover, it was found that different passive mixers such as T type and Y type are used to improve mixing of immiscible liquids in channels. These have simple system design with a reasonable mixing efficiency [24]. The performances such as mixing efficiency and pressure losses of a microchannel depend on the type of flow patterns which are developed in the microchannel. These flow patterns give an idea about the specific interfacial area available for mass transfer. The flow pattern generated at a microfluidic junction depends on the geometry of the microfluidic mixer or junction [25]. Consequently, the knowledge of the flow pattern produced in a specific mixer is important while designing any process. There are limited data reported in the literature on mixing performance and pressure loss data for these types of mixers with small diameter [24-27]. These gaps in literature motivated us to investigate the effect of two different mixers on the overall pressure losses in the coiled tube system. Therefore, an experimental study was carried out to investigate the liquid-liquid flows through coiled tubes with a small diameter at lab scale. The effects of velocity of oil and water, oil volume fraction and type of mixer (T and Y type) on the pressure drop for an oil-water flow in a coiled tube of diameter 7 mm were experimentally studied.

Knowledge of pressure drop will help in evaluating the energy losses through these types of systems. It is important to identify the flow pattern as it aids in identifying the multiphase flow behaviour and designing of process equipment. Therefore, the flow patterns observed at different velocities of oil and water were reported here.

MATERIALS AND METHODS

Fig. 1 shows the experimental set-up in which the present work was carried out.
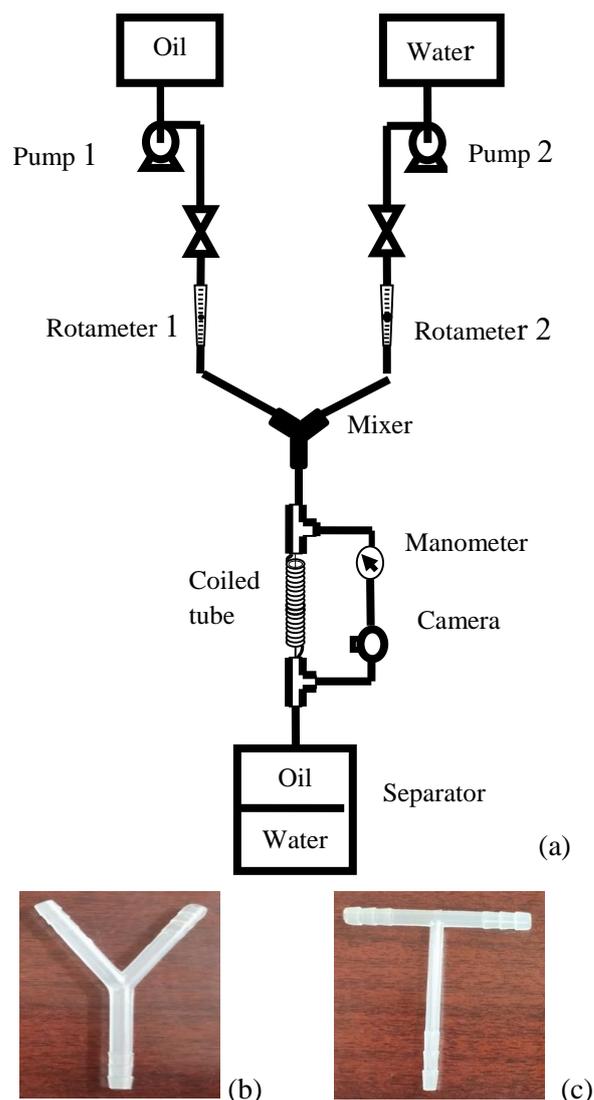
Fig. 1. (a) Experimental set-up, (b) Y type mixer, (c) T type mixer

The facility consists of two storage tanks which were used for containing oil (kerosene) and water, respectively. The experiments were conducted at an ambient temperature of 27–28 °C. The properties of kerosene and water are shown in Table 1. The two liquids were pumped with two pumps whose maximum flow rate was 1.5 m/s.

Table 1. Properties of liquids

Fluids	Kerosene	Water
Density, kg/m^3	800	996
Dynamic viscosity, Pa-s	0.00164	8.9×10^{-4}
Interfacial tensions @ 20 °C, mN/m	Water /kerosene	23

The kerosene and water flow rates were measured by independent rotameters, with a measuring range of 0-2 lpm, corresponding to a superficial velocity range of 0-0.9 m/s, and uncertainty, obtained *via* calibration, of ±1% of full scale value. Acrylic rotameters were used to measure water and kerosene flow rates. The rotameters were factory-calibrated for given liquids under given ambient temperature and pressure conditions. These devices were re-calibrated to ensure that accurate measurements are taken. A T-type or Y-type mixing section was connected to mix the kerosene and water. The pictures of the mixers are shown in Fig.1 (b) and (c). The liquids then entered the test section (coiled tube). The test section was a transparent PVC tube with a diameter of 0.007 m and length of 89 cm which was tightly coiled over different cylinders for obtaining different curvature ratios (ratio of diameter of coiling to diameter of tube, λ=dc/dt). The coil curvature ratios were 5, 7 and 28. The experiments were carried out with superficial velocity of the liquids ranging from 0.04 m/s to 0.4 m/s. Investigations on various water and kerosene volume fractions were carried out by adjusting their flow rates. A U-tube manometer containing mercury was connected just near the inlet and outlet of the coiled tube to determine the pressure drop of the immiscible liquids flowing in the coiled tube. In the present work, total pressure drop was calculated from eq. (1):

$$(\Delta P_T) = \rho g (\Delta h) \tag{1}$$

Here ρ is the difference in density of mercury in manometer and density of oil-water mixture. Δh is the difference in height of mercury in manometer observed during the experimentation and g is the acceleration due to gravity.

The total two-phase flow pressure losses are considered to be the sum of pressure losses due to friction (ΔP_{fric}), pressure losses due to acceleration ($\Delta P_{acceleration}$) and hydrostatic pressure loss:

$$(\Delta P_{static}). \ \Delta P_T = \Delta P_{fric} + \Delta P_{acceleration} + \Delta P_{static} \tag{2}$$

Acceleration pressure losses ($\Delta P_{acceleration}$) may be considered to be negligible for isothermal flows in constant-diameter tubes. In eq. (2), the hydrostatic pressure loss is:

$$(\Delta P_{static}) = \rho_{mix} g \sin\varphi l \tag{3}$$

where l is the difference in elevation of inlet and outlet of the coiled tube and φ is the angle of flow. Therefore, the pressure drop due to frictional losses, (ΔP_{fric}), can be estimated from eq. (4):

$$(\Delta P_{fric}) = (\Delta P_T) - (\Delta P_{static}) \tag{4}$$

Moreover, the friction factor, *f*, can be calculated from eq. (5):

$$(\Delta P_{fric}) = 2 \frac{f U_{mix}^2 \rho_{mix}}{d} L \tag{5}$$

Here L is the length of coiled tube and d is the internal tube diameter. The properties of the oil-water mixture were calculated based on their individual properties and volume fractions of the immiscible liquids [10]. Density of mixture, ρ_{mix}, was calculated by equation (6):

$$\rho_{mix} = \rho_o \, \varphi_o + (1 - \varphi_o) \rho_w \tag{6}$$

where the volume fraction of oil, $\varphi_o = \frac{\text{inlet oil flowrate}}{\text{total liquid flowrate}}$, ρ_o is density of oil, ρ_w is density of water. The mixture velocity, U_{mix}, is the sum of both phases' superficial velocities:

$$U_{mix} = U_{sw} + U_{so}, \tag{7}$$

where U_{sw} and U_{so} correspond to water and oil superficial velocities, respectively. Friction factor, f, was calculated from eq. (5) and then plotted against Reynolds number, Re. Re can be calculated from equation (8):

$$Re = \frac{d \rho_{mix} U_{mix}}{\mu_{mix}} \tag{8}$$

Here the viscosity of the mixture, μ_{mix} was calculated based on the volume fraction of oil, φ_o, viscosity of oil, μ_o, and viscosity of water, μ_w, as given in eq. (9):

$$\mu_{mix} = \mu_o \, \varphi_o + (1 - \varphi_o) \mu_w \tag{9}$$

Each run continued for some time to achieve a steady-state flow before acquiring and recording the experimental data. The oil-water mixture was subsequently passed to a tank for separation of the oil and water. The pictures of the various patterns of flow at different velocities were taken using a digital camera Nikon 5300D. Concentrated dye soluble in the oil or water phase was added into the feed tanks for better visualization of flow patterns. The

389

selection criterion of dye was its solubility in one phase only. Fluorescein Sodium (green in color) was chosen as the dye for water and Biebrich Scarlett R (red in color) was chosen for the oil phase.

RESULTS AND DISCUSSION

In the present study, oil and water superficial velocities were varied from 0.04 to 0.4 m/s. Different patterns of flow were observed at varying velocities.

(a)   (b)   (c)

(d)   (e)   (f)

(g)
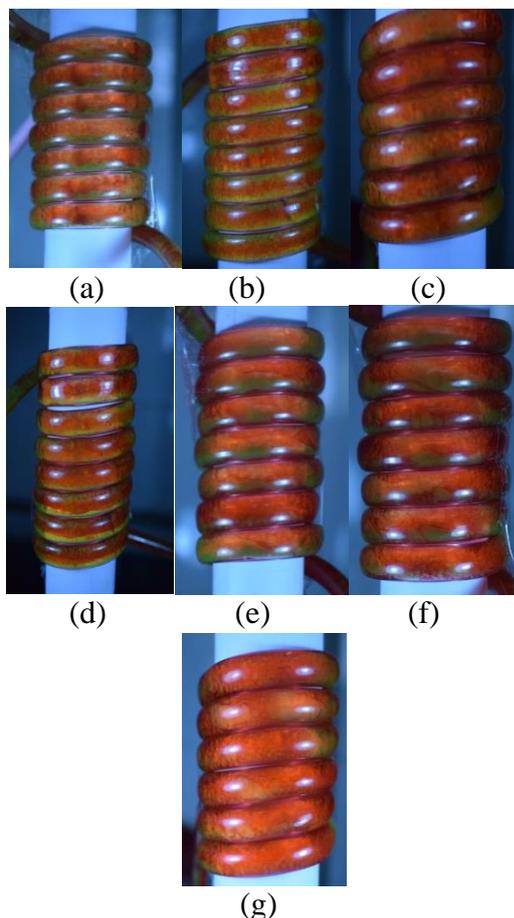
Fig. 2. Different flow patterns observed in the present study (a) Oil dispersed in water over a water layer, Do/w &w, Vos = 0.04 m/s, Vws = 0.39 m/s; (b) annular flow, A, Vos = 0.13 m/s, Vws = 0.39 m/s; (c) Oil in water emulsion, Eo/w, Vos = 0.17 m/s, Vws = 0.30 m/s; (d) stratified flow, ST, Vos = 0.21 m/s, Vws = 0.30 m/s; (e) Wavy stratified flow, WST, Vos = 0.26 m/s, Vws = 0.17 m/s; (f) Water dispersed in oil under an oil layer, Dw/o &o, Vos = 0.30 m/s, Vws= 0.12 m/s; (g) water in oil emulsion, Ew/o, Vos = 0.30 m/s, Vws = 0.04 m/s.

Following patterns were noted:

(a) Oil dispersed flow (Do/w &w): Tiny oil droplets were dispersed in water over water layer;

(b) Annular flow (A): oil drops were dispersed in core and water in the annulus region of the coiled tube;

(c) Emulsion flow (Eo/w): oil drops were distributed in the continuous water phase;

(d) Stratified flow (ST): oil and water flow in separate layers;

(e) Wavy stratified flow (WST): wavy interface is observed between separate layers of oil and water flow;

(f) Water dispersed flow (Dw/o &o): Water droplets are dispersed in oil under oil layer;

(g) Emulsion flow (Ew/o): water drops are distributed in the continuous oil phase.

Fig. 2 shows the pictures of different flow patterns of oil in the coiled tube with a diameter of 0.007 m. The figure is arranged sequentially with increase in velocity of oil and decrease in velocity of water. Fig. 2 (a) shows the flow pattern when the velocity of oil is least, i.e. 0.04 m/s while the water velocity is maximum, i.e. 0.39 m/s. It can be observed that oil bubbles are dispersed in water at the upper section of coiled tube. When the velocity of oil increases to 0.13 m/s, the flow pattern changes to annular flow. Fig. 2(b) depicts that the oil is dispersed at the core while water is at the annulus of the tube. Fig. 2(c), shows that as superficial velocity of oil is increased to 0.17 m/s while the water velocity is decreased to 0.3 m/s, water is in continuous phase and oil bubbles are distributed throughout the tube cross-section. Stratified flow is viewed at oil velocity of 0.21 m/s and velocity of water of 0.3 m/s. This is illustrated in Fig. 2 (d). The first five turns of the coiled tube have a stratified flow with mixed interface. The last three turns of the coil tube have a more distinct interface between the immiscible liquids. The interface between the two immiscible liquids is clear cut, smooth and displays two noticeable separate regions of different liquids. Fig. 2 (e) shows that the increase in superficial velocity of oil to 0.26 m/s and decrease in velocity of water to 0.17 m/s lead to a wavy stratified flow. The additional enhancement in velocity of oil (0.30 m/s) leads to a change in flow pattern in which water is dispersed in oil under the oil layer. This is revealed in Fig. 2 (f). In this case, the continuous phase is oil. When the water velocity is decreased to 0.04 m/s, water bubbles are found to be dispersed in the oil as shown in Fig. 2 (g). Hence, it is observed that changes in velocity of oil and water affected the pattern of flow. These flow patterns were plotted for varying water and oil velocities and are illustrated in Fig. 3. Figures 3 (a) and 3(b) show the flow pattern maps for T type mixer and Y type mixer, respectively. The figure exemplifies the flow regime of the oil-water flow through a coiled tube with curvature ratio of 5.

Fig. 3(a) illustrates that in the T type mixer, flow pattern Do/w (oil dispersed in water) was observed for the mixture where water was at a higher velocity of 0.4 m/s and oil was at a lower velocity of 0.04 m/s. Gradually, annular flows were observed when the oil velocity was increased to around 0.1 m/s and water velocity was still higher at 0.35 m/s. Stratified flow and wavy stratified flows were observed when the oil and water velocities were in similar ranges. Emulsion of water in oil was observed when the water velocity was low (0.04 m/s) as compared to oil. Fig. 3 (b) shows the flow pattern map for the Y type mixer. It can be seen from Fig. 3 (b) that some of the flow patterns such as annular, stratified, as well as emulsion of water in oil were not detected for the present experimental conditions in the Y type mixer. At low oil velocity (0.17 m/s) and higher water velocity, dispersion of oil over water layer was observed.
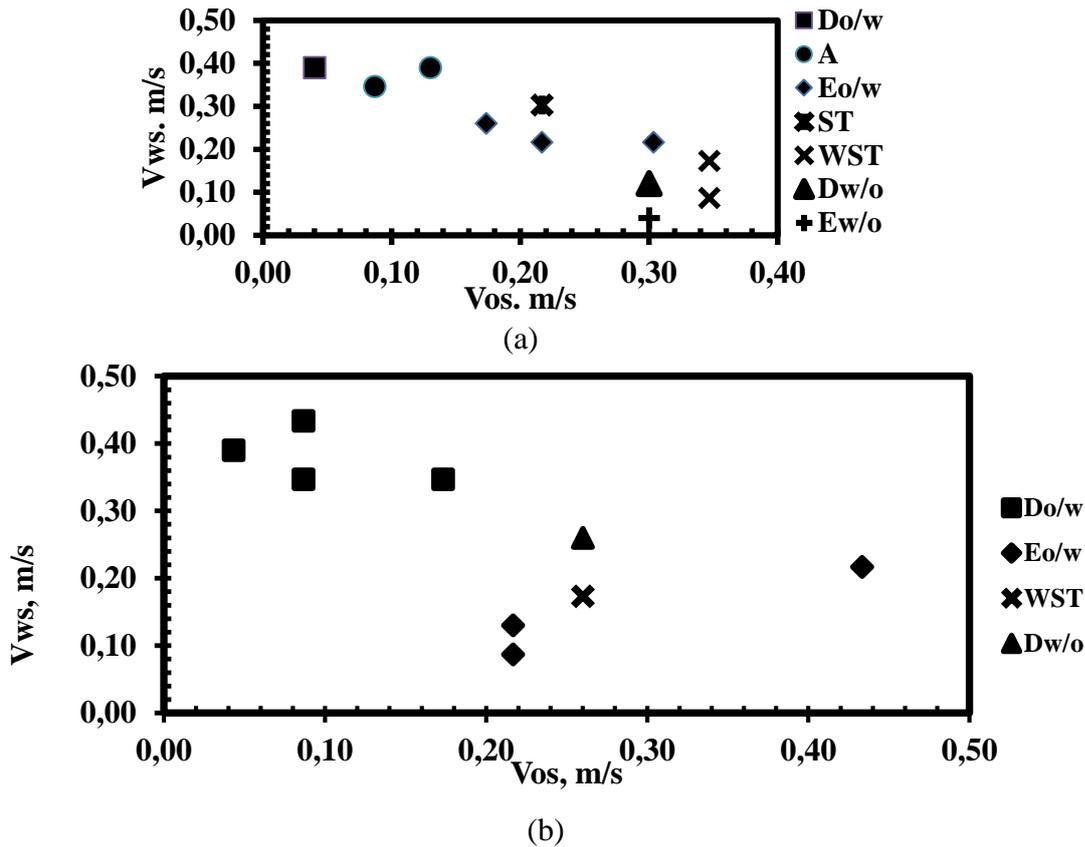

(a)

(b)

Fig. 3. Flow regime of the oil water flow through a coiled tube with d_t=0.007 mm, λ=5
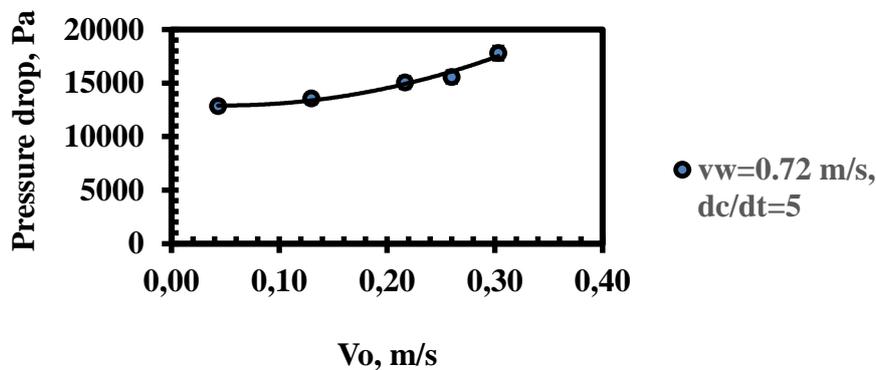(a) T type mixer, (b) Y type mixer

Fig. 4. Pressure drop *vs.* velocity of oil through the coiled tube of diameter 0.007 m, λ=5 at constant water flow rate of 0.72 m/s

Emulsion of oil in water was observed when the oil velocity was increased to 0.21 m/s. Wavy stratified flow pattern was found when the oil velocity was further increased to 0.26 m/s. Dispersion of water under the oil layer was found when velocities of both water and oil were 0.26 m/s.

Fig. 4 shows the values of pressure drop at various oil velocities. The velocity of oil was varied within the range of 0.04 to 0.3 m/s and water velocity was kept constant at 0.72 m/s. Pressure drop was found to be increasing with increase in oil velocity. When the oil velocity was increased from 0.04 to 0.3 m/s, there was nearly 25 % enhancement in pressure drop. This is due to the enhancement of inertial forces with increasing flow rates. Parity plots were plotted for pressure drop values measured from the present experiments against values predicted for single-phase flows in a coiled tube from correlations of Mishra and Gupta (1979) [28] and are shown in Fig. 5.
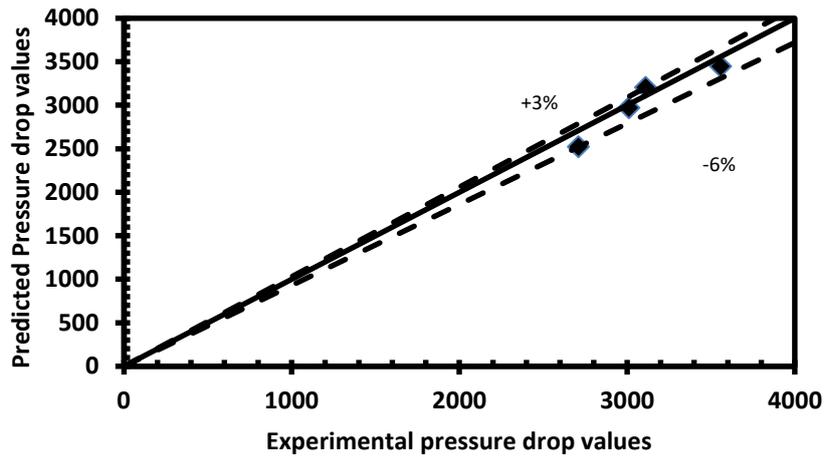

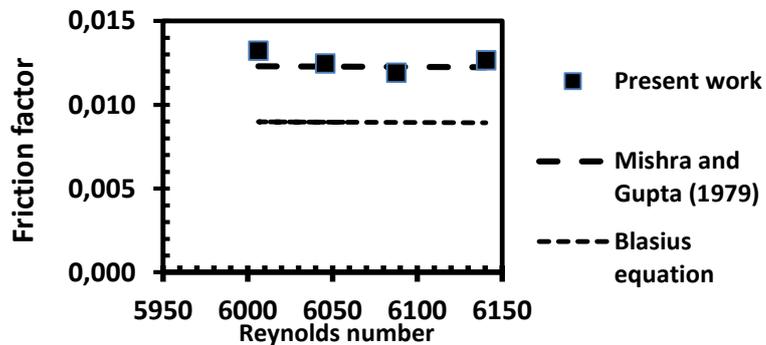**Fig. 5.** Parity plot of experimental pressure drop values *vs.* predicted pressure drop values

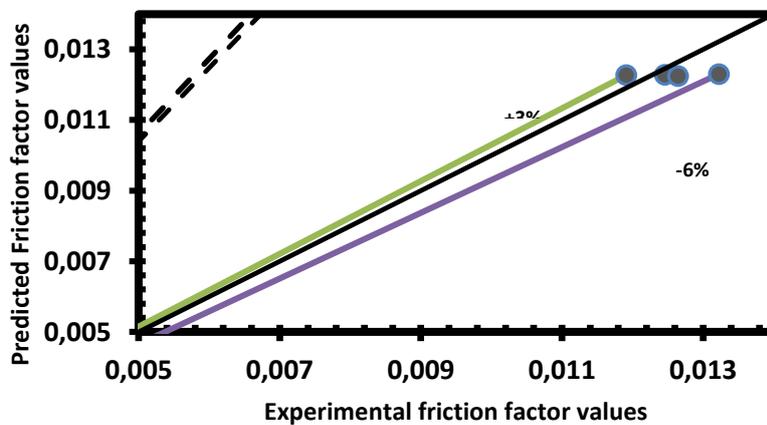**Fig. 6.** Comparison of friction factor *vs.* Reynolds number with previous literature

Fig. 7. Parity plot of experimental friction factor values *vs.* predicted friction factor values

The friction factor values were calculated for different Reynolds numbers and are reported in Fig. 6. The present data were compared with existing correlations previously reported for single-phase flows in a coiled tube, as well as in a straight tube by Mishra and Gupta (1979) [28] and by Blasius equation [29], respectively. It was found that under present flow conditions, the friction factor decreased with the increase in Reynolds number. Friction factor calculated from the present work was found to be by 24 to 32 % higher than that of Blasius equation proposed for a straight tube. Present experimental values were found to be in agreement with values predicted by correlation of Mishra and Gupta (1979) [28]. Fig. 7 shows the parity plot between friction factor values calculated from present experiments and values predicted from correlations of Mishra and Gupta (1979). Present experimental values are in

agreement with predicted values and are within ±6 % error.

Fig. 8 shows the effect of oil fraction on pressure drop across the coiled tube with a curvature ratio $d_c/d_t=7$. Pressure drop increased with the increase in both oil fraction and velocity of oil-water. This was because of the enhancement of overall viscous forces and inertial forces. The percentage increase in pressure drop for the different velocities was 10 % at 0.3 oil fraction. However, this increment was 20 % for 0.5 oil fraction. The effect of curvature ratio on pressure drop at different oil fractions can be seen in Fig. 9. The curvature ratios were 7 and 28. The difference in pressure drop due to varying curvature at 0.41 oil fraction for 0.43 m/s was nearly 9 %. However, the increment increased to 25 % for v=0.52 m/s at oil fraction of 0.75.
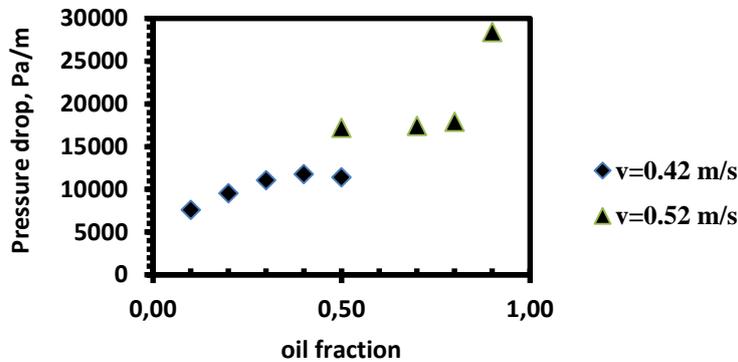

Fig. 8. Variation of pressure drop and oil fraction for different mixture velocities for d_t=0.007mm, λ=7
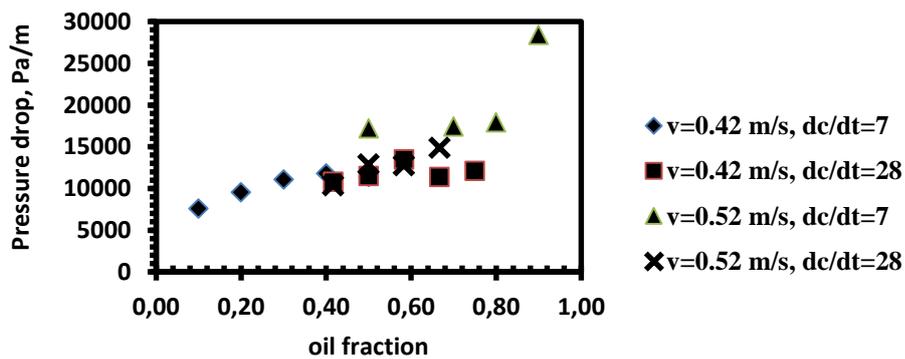

Fig. 9. Pressure drop *vs*. oil fraction for different curvature ratios
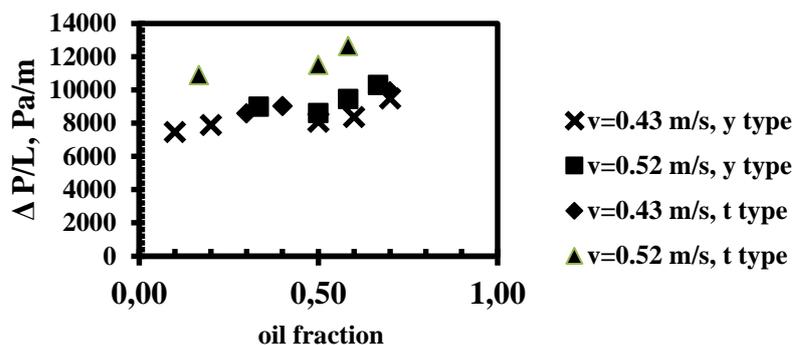
Fig. 10. Pressure drop *vs*. oil fraction for T-type mixer and Y- type mixer

This shows that the effect of curvature ratio on pressure drop was prominent at higher velocity. This was because of stronger development of secondary forces in a coiled tube at higher velocity.

Literature shows that the type of mixers has impact on the flow patterns of liquids flowing in micro tubes. The effect of two types of mixers (T type and Y type) on pressure drop was investigated and displayed in Fig. 10. In the present work, no significant effect was observed for lower velocity. However, pressure drop was found to increase for higher velocity (v=0.52 m/s) when the liquids flow through a T type mixer. Pressure drop value was by nearly 26 % higher in T type as compared to Y type mixer.

CONCLUSIONS

The present experimental study was carried out to gain insight on the hydrodynamics of oil-water flows through a coiled tube of diameter 7 mm. The study helped in identifying the various flow patterns of two immiscible liquids, i.e. kerosene and water. Various patterns of flow such as stratified, dispersed and annular flows were observed at different superficial velocities of water and oil. Flow pattern maps were plotted based on varying water and oil superficial velocities and reported for T type and Y type mixers. Effect of parameters such as velocity of oil, curvature ratio of coiled tube and oil fraction on pressure drop was observed. It was found that there was nearly a 25 % increment in pressure drop as the total oil–water flow velocity was increased from 0.76 m/s to 1.1 m/s. The influence of curvature of coiled tube on pressure drop was prominent at higher velocities. There was a pressure drop increment of 25 % for oil fraction of 0.75 at velocity 0.52 m/s. Increase in oil fraction lead to an increase in pressure drop due to enhancement of viscous forces. The significance of T or Y type mixer on pressure drop was observed for higher velocity. The T type mixer produced 26 % higher pressure drop for the oil-water flow with v=0.52 m/s in the coiled tube. This

suggests that Y type mixers may be preferred to minimize energy losses for oil-water flows. Present study will be helpful in designing energy-efficient reactors and heat exchangers where immiscible liquids are used.

REFERENCES

1. H. Alboudwarej, J. Felix, R. Badry, *Oilfield Review*, **18 (2)**, 34 (2006).
2. X. Luo, G. Lü, W. Zhang, L. He, Y. Lü, *Exp. Therm. Fluid. Sci.*, **82**, 174 (2017).
3. M. Dongjun, L. Gensheng, H. N. Mingjuan, L. Jingbin, *Petrol. Explor. Develop.*, **39**, 528 (2012).
4. A. Abdollahi, R. N. Sharma, A. Vatani, *Int. Commun. Heat Mass*, **84**, 66 (2017).
5. R. Kaur, M. Ramakrishna, K.D.P. Nigam, *Rev. Chem*, **23**, 247 (2007).
6. R. Kaur, M. Ramakrishna, K.D.P. Nigam, *Int. J. Chem. React. Eng.,* **5**, A27 (2007).
7. T. K. Mandal, D. P. Chakrabarti, G. Das, *Chem. Eng. Res. Des.*, **85(8),** 1123 (2007).
8. P. Angeli, G. F. Hewitt, *Int. J. Multiph*ase **24**, 1183 (1999).
9. N. Brauner, *Int. J. Multiph*ase, **27**, 885 (2001).
10. M. Hadziabdic, R. V. A. Oliemans, *Int. J. Multiph*ase, **33**, 1365, (2007).
11. J. Jing, J. Sun, J. Tan, M. Huang, Q, Liang, T. Xue, *Exp. Therm. Fluid Sci*., **72**, 88 (2016).
12. A. Mukhaimer, A. Al-Sarkhi, M. El Nakla, W.H. Ahmed, L. Al-Hadhrami, *Int. J. Multiph. Flow*, **100 (73)**, 90 (2015).
13. E. L. Guajardo, E. O. Nadal, E. M. Castellanos, K. D. P. Nigam, *Chem. Eng. Sci.*, **169**, 179 (2017).
14. M.M. Mandal, C. Serra, Y. Hoarau, K. D. P. Nigam, *Microfluid Nanofluid*, **10**, 415 (2011).
15. E. A. López-Guajardo, G. M. Garza-Cantú, A. Marques-Camarena, E. Ortiz-Nadal, K. D. P. Nigam, A. Montesinos-Castellanos, *Ind. Eng. Chem. Res.*, **58**, 1075 (2019).
16. M.M. Mandal, P. Aggarwal, K. D. P. Nigam, *Ind. Eng. Chem. Res.*, **50(23)**, 13230 (2011).

17. M. Darekar, K. K. Singh, S. Mukhopadhyay, K. T. Shenoy, *Eng. Chem. Res*., **56 (42)**, 12215 (2017).
18. T. Ganat, S. Ridha, M. Hairir, J. Arisa, R. Gholami, *J. Petrol. Explor. Prod. Technol.*, **9**, 2911 (2019).
19. M. Du, N .D. Jin, Z. K. Gao, Z. Y. Wang, L. S. Zhai, *Int. J. Multiph. Flow*, **41**, 91 (2012).
20. H. Hu, J. Jing, J. Tan, G. H. Yeoh, *Exp. Comput. Multiph. Flow,* **2**, 99 (2020).
21. T. Al-Wahaibi, Y. Al-Wahaibi, A. Al-Ajmi, R. Al-Hajri, N. Yusuf, A. S. Olawale, I. A. Mohammed, *J. Petrol. Sci. Eng.*, **122**, 266 (2014).
22. L. Edwards, D. Jebourdsingh, D. Dhanpat, D. P. Chakrabarti, *Cogent Eng*., **5**, 1494494 (2018).
23. A. Dey, M.M. Mandal, *Adv. Sci. Eng. Med*., **12**, 173 (2020).
24. S.S. Hsieh, J.W. Lin, J.H. Chen, *Int. J. Heat Fluid Fl.,* **44**, 130 (2013).
25. S. Sarkar, K. K. Singh, V. Shankar, K. T. Shenoy, *Chem. Eng. Process*, **85**, 227 (2014).
26. S. M. Tu, S. Torii, Y. C. Shi, *J. Multiphysics*, **5**, 215 (2011).
27. L. Xin, W. Shaoping, *CJA*,**26(4)**, 1080 (2013).
28. P. Mishra, S. N. Gupta, *Ind. Eng. Chem. Process Des. Dev.*, **18**, 130 (1979).
29. W. L. McCabe, J. C. Smith, P. Harriott, Unit operations of chemical engineering (5th edn.). New York, London, McGraw-Hill, 1993.